

On the Fly Ellipsometry Imaging for Process Deviation Detection

T. Alcaire¹, D. Le Cunff², S. Soulan, and J.-H. Tortai

Abstract—Spectroscopic ellipsometry is a very sensitive optical metrology technique commonly used in semiconductor manufacturing lines to accurately measure the thickness and refractive index of different layers present on specific dedicated metrology targets on the wafers. In parallel, optical defectivity techniques are widely implemented in production lines to inspect a significant amount of dies representative of the full wafer and detect physical and patterning defects. A new approach can then simply emerge which is to apply ellipsometry metrology techniques at a full or die wafer scale. This strategy, at the frontier between metrology and defectivity field is expected to bring solutions for certain types of process deviation. In our case, ellipsometry's optical response was collected on large areas of product wafers to capture specific deviations such as film properties, thickness, and patterning variation. This is an innovative strategy that relies on a model-less approach to detect process drifts, using ellipsometry's sensitivity to material properties and design architecture variations. In this paper, we will present this approach on three industrial cases.

Index Terms—Model-less, metrology, defectivity, process control, ellipsometry imaging.

I. INTRODUCTION

IN THE standard approach, Spectroscopic Ellipsometry (SE) is used to measure the thicknesses and optical indices of multistack layers deposited on a substrate with models based on Fresnel laws. When ellipsometers are used for scatterometry purpose through modeling of the scattering of light on a periodical patterned structure, it is referred as Optical Critical Dimension (OCD) control. Both applications require a detailed knowledge of the layers and/or of the structure constituting the metrology targets in order to develop a realistic mathematical model. By simulating the spectroscopic ellipsometry response and after a reverse

problem-solving operation, one can then extract the parameters of interest (thickness, optical indices, critical dimensions, side wall angles and more). This model-based process can be very time consuming and request heavy engineering effort (pre-characterization, cross comparisons...). Typically, both ellipsometry and OCD control also require the design of specific blanket or periodical targets on sacrificial areas of the product wafer.

In recent years, in order to accelerate the learning curve in new technological introduction, but also to develop metrology target structures more representative of the device, model-less strategy have been introduced in the metrology field [1], [2]. Indeed, raw measurements of ellipsometers, especially on real time mode, are in essence extremely sensitive to slight variation of thicknesses (down to some Angstrom), slight optical index variation (down to 0.01 variation in n values) and patterning details (shape, dishing...). The recent adoption of Artificial Intelligence (AI) concepts supported by Machine Learning or Deep Learning algorithms has accelerated this trend. In this paper, we propose to explore the benefit of ellipsometry acquisitions over the full wafer surface combined with an advanced data treatment. Indeed, the complexity of the optical ellipsometry response from the underlying design structure of a product wafer inevitably leads to the implementation of a model-less approach to detect local process deviation. Even though industrial imaging ellipsometry solutions exist [3], they tend to only study small uniform layers in order to be able to obtain thickness or indexes values, therefore requiring a rigorous model development.

The approach described in this study consists in reconstructing an image of the wafer, channels of the image being the raw ellipsometry data measured on the fly during a controlled stage displacement without any modeling and then applying a data treatment analysis. Three cases of process deviation detection at a wafer scale are studied in this paper.

II. EXPERIMENTAL SETUP AND PROTOCOL

In this section, we describe the spectroscopic ellipsometry (SE) equipment that was used for this study as well as the protocol for ellipsometry acquisition and image generation.

A. Spectroscopic Ellipsometer

SE metrology industrial equipments are completely inappropriate for scanning a full wafer surface. They provide point-based measurements so mapping a whole wafer surface with a high-resolution grid will last far too long. Industrial SE

Manuscript received 15 February 2022; revised 4 May 2022 and 8 June 2022; accepted 10 June 2022. Date of publication 15 June 2022; date of current version 4 August 2022. This work was supported in part by the Electronic Component Systems for European Leadership Joint Undertaking Project MADEin4 under Grant 826589, which receives support from the European Union Horizon 2020 Research and Innovation Program and, Austria, Belgium, France, Germany, Hungary, Ireland, Italy, The Netherlands, Romania, and Sweden; and in part by the French ANR Program Investissements d'Avenir EQUIPEX under Contract ANR-10-EQPX-33. (Corresponding author: T. Alcaire.)

T. Alcaire and D. Le Cunff are with STMicroelectronics, 38926 Crolles, France (e-mail: thomas.alcaire@st.com; delphine.le-cunff@st.com).

S. Soulan and J.-H. Tortai are with LTM/CNRS, CEA-LETI, Grenoble, France (e-mail: sebastien.soulan@univ-grenoble-alpes.fr; jean-herve.tortai@ltmlab.fr).

Color versions of one or more figures in this article are available at <https://doi.org/10.1109/TSM.2022.3183257>.

Digital Object Identifier 10.1109/TSM.2022.3183257

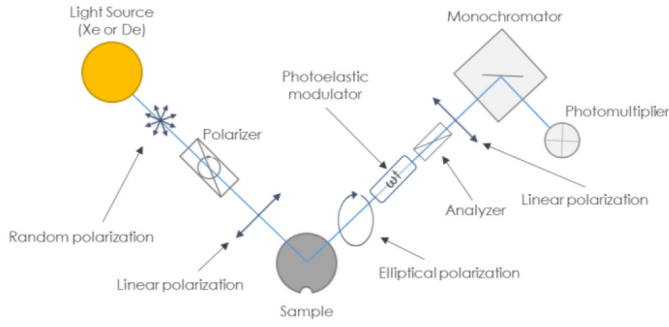


Fig. 1. Schematic of the phase-modulated ellipsometer working principle.

equipments are dedicated to measure a limited number of target structures on the wafer surface, the spot size being small enough to fit entirely inside the dedicated structures ($< 30 \mu\text{m}$ size). On another hand, academic SE equipments are often designed to measure thickness and optical index materials with high accuracy but with larger spot sizes ($> 100 \mu\text{m}$), regarding less the measurement throughput. Among ellipsometry technologies, phase modulated ellipsometers are good candidates for academic studies as, by its principle, the measurement gain is not dependent of the measured wavelength thanks to the photomultiplier detector. In addition, the spectroscopic scan can be tuned at will thanks to the use of a monochromator. The drawback of this configuration is a slow acquisition time for a spectroscopic scan (> 2 minutes for 100 measured wavelength) as it is measured sequentially by the monochromator. Nevertheless, if a single wavelength is selected by the user, kinetic measurements are possible, and the measurement rate is high (acquisition periods $< 25\text{ms}$) thanks to the time response of the Photomultiplier and to the high modulation frequency of the Photo Elastic Modulator ($f \approx 50\text{kHz}$). In this paper, we used an academic phase-modulated ellipsometer whose basic schematic is presented in Fig. 1, and the exact configuration can be found in [4]. For phase-modulated ellipsometer, the raw data gathered are the ellipsometry parameters I_s and I_c , which values are bound between -1 and 1 . These are linked to the usual ellipsometric angles Δ and Ψ through equations (1) and (2).

$$I_s = \sin(2\Psi) \sin(\Delta) \quad (1)$$

$$I_c = \sin(2\Psi) \cos(\Delta). \quad (2)$$

The ellipsometer used in this paper is an inline UVISEL 2 (IMPACT platform), which covers a large broadband spectrum ($150\text{nm} - 2\mu\text{m}$) thanks to two light sources, a Xenon, and a Deuterium lamp, and is able to collect responses at any coordinates on the surface of a 300mm wafer at a fixed incident angle of 70° . It is capable of gathering kinetic data, allowing for acquisition frequency up to 100 Hz . Various spot sizes can be set, the smallest one being $300 \times 300 \mu\text{m}$. This research tool is dedicated to the characterization of advanced materials deposited onto 300mm and wafers loading are handled by an automated transfer chamber and 300mm wafer carriers connected to various process equipment (Plasma etching chambers, ALD chambers). The whole transfer from equipment to IMPACT ellipsometer is achieved under vacuum to

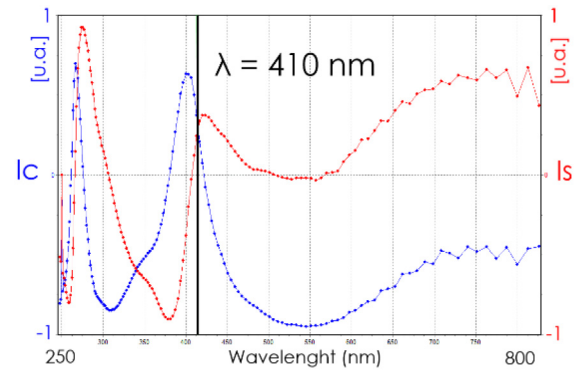


Fig. 2. Example of spectroscopic scan used to determine the optimal wavelength.

prevent any surface contamination or oxidation. In a standard operating mode, 300 mm mapping capability is possible using point-to-point measurements. But, by choosing a single wavelength, a full wafer image can be reconstructed by using a new on fly acquisition routine that will be described later. The scanning time of the wafer is still long compared to industrial defectivity tools ($2-4$ hours depending on the image resolution) but is reasonably fast especially regarding the number of pixels in the image (from thousands of points up to 1.5 million measured pixels). A conventional mapping strategy with so many points will last days at minimum. The wavelength used for the image reconstruction is chosen by analyzing the variation of the recorded signature of a spectroscopic scan on a region of interest of the wafer. The criteria for the choice of the recorded wavelength for the image reconstruction is a high local variation of both recorded channel I_s and I_c .

B. Acquisition Protocol and Image Generation

A specific ellipsometry image reconstruction protocol was implemented for data acquisition and treatment. As a preliminary step, a spectroscopic survey is performed to select an arbitrary optimum wavelength to get maximum sensitivity to the given process deviation.

1) *Survey Scan and Wavelength Selection:* The first step of the protocol consists in performing a spectroscopic ellipsometry scan in the area of interest/a typical die using a larger spot to obtain its average optical signature. The resulting spectrum is useful to choose the single wavelength that will be further selected to perform a large scale I_s and I_c raster acquisition. The basic approach we used was to choose the optimal wavelength for which both I_s and I_c curves intercept and if multiple candidates emerge, to select the one with the highest local slopes (Fig. 2). The reason behind this arbitrary assumption is that two channels are recorded (I_s and I_c) and any small variations of the optical properties of the sample should result in large variations on both I_s and I_c components, the intercept normalizing the initial pixel value.

In order to increase the reliability of the wavelength protocol selection, another alternative based on virtual substrate was explored. A spectroscopic survey is performed in the same region of interest before and after the process step of

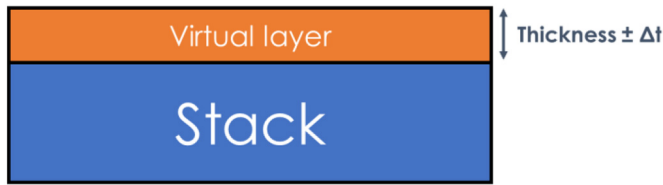


Fig. 3. Schematics of structure considered for the evaluation of signal variation induced by a small thickness variation of the virtual layer, allowing for the optimal wavelength selection.

interest. Indeed, by using the first spectrum (before the process step) as a basis, we can use the second one to create a virtual effective layer. This layer then represents the variation in the optical properties induced by the process step. The virtual material thus can be used to simulate layers of varying thicknesses or roughness. The optical response variation induced by these variations allows for the selection of the optimal wavelength where raw data exhibit the highest sensitivity. This is evaluated by measuring the signal variation of both I_s and I_c and selecting the wavelength where the highest change is located. Also, by measuring the same region twice, we remove any underlying stack variations and any optical response variations is therefore due to the last process step. For heavily inhomogeneous process steps, where material properties could vary strongly between different regions of the wafer, this approach could be applied to multiple sites in order to obtain a wavelength sensitive to variations on the full wafer surface.

2) *Data Acquisition*: In a very basic approach, to gather ellipsometry data of a large region of interest, successive measurements on a dense mapping grid was implemented (Fig. 4a). This was then only suitable for process deviations inducing large signatures.

One asset of the IMPACT ellipsometer is to allow gathering data on the fly during the stage displacement by using a *Raster* scanning mode, each point being recorded in a kinetic mode by synchronizing the data saving. This is illustrated in schematics in Fig. 4b. This is, to our knowledge, the first application of this kind that has been published. This mode allows faster acquisition and better resolved image compared to classical point-to-point mapping strategy.

For the practical usage, certain parameters must be set, such as starting and ending X and Y coordinates, limiting the possible scannable areas to rectangular shapes. The acquisition sequence is simple : the ellipsometer scans along the X axis, shift its Y coordinate at the end of every line, as is shown in Fig. 4b. The time interval between measurements (X resolution) and number of lines (Y resolution) can be set based on the final desired image resolution. The time interval was chosen here to record every pixel at a distance corresponding to the spot size (one pixel every 300 μm in X and Y directions). One must keep in mind it is possible to overlap pixels without a drastic scanning duration impact. Unfortunately, the stage of this academic equipment is not originally intended to be used in a continuous scanning mode.

The motors are designed to move sequentially and not in a raster mode (continuous displacement at a controlled velocity)

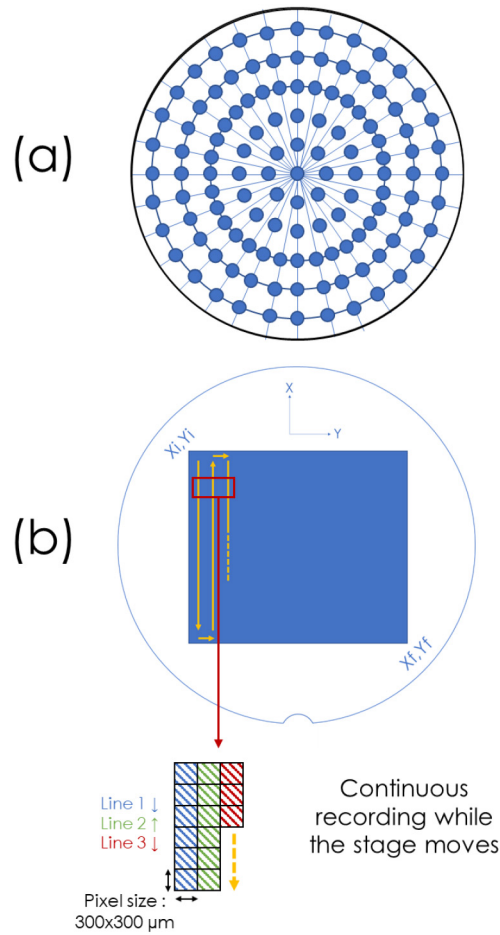


Fig. 4. (a) Typical mapping used for point-to-point basic measurements and (b) Raster scanning scenario of the wafer, local dense pixelization with the 300x300 μm spot and full dense scan of a large area with 300x300 μm recorded “pixels”.

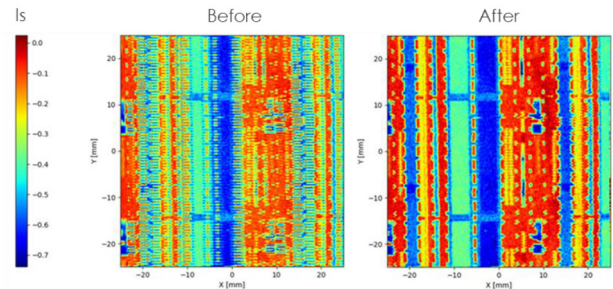


Fig. 5. Ellipsometry images before (left) and after (right) corrections of the aberrations done by the Python script (only I_s represented here).

and conversely exhibits measurements artifacts due to gripping points of the wafer holder and slight variations of the displacement velocity. These gripping points and local velocity variation induce wrong calculated position with time during the stage displacement and positioning error that must be compensated for (Fig. 5a).

To get rid of these aberrations, a Python script was created which automatically corrects the X positions of each line by shifting all the X values with an optimized constant bias and

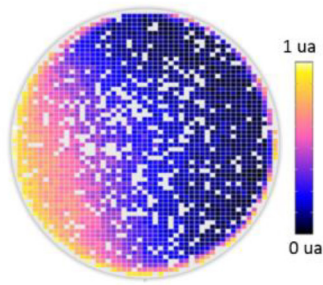


Fig. 6. Normalized Electrical Yield wafer map of dies showing a diametrical intra-wafer signature (White : no test result – 0 is good, 1 is bad).

by adding local corrections to compensate for erratic stage displacement during the scan. This is done by comparing adjacent lines and finding the optimal X-shift, defined by the smaller gradient across them. Finally, once the position are corrected, a well resolved ellipsometry images is generated (Fig. 5b), considering the equipment used in this study was not designed for this type of acquisitions. This image is then compared with full wafer optical images to check the validity of our corrections.

3) *Image Generation*: Ellipsometry images are generated by assigning each value of I_s and I_c measured at a given wavelength to their corresponding X and Y coordinates, and therefore the outcome consists in two ellipsometry images of the region of interest. For the basic point-to-point measurements, the images are obtained after performing a cubic interpolation to complete missing data between the measured points. This was implemented using a custom-written Python script. This interpolation step was therefore not necessary when using the raster mode, where the entire region studied is acquired on the fly.

III. RESULTS

This section describes the results obtained conducting the acquisition protocols previously presented on three cases of process variation: *i) Intra-wafer nitride passivation layers properties variation* using the basic point-to-point acquisition protocol, *ii) Color resist layers intradie thickness variation*, and *iii) Periodic etched 3D structures critical dimensions variation* applying the raster mode respectively.

A. Intra-Wafer Nitride Passivation Layers Properties Variation

For the first use case, we tested the sensitivity of our model-less ellipsometry approach to detect intra wafer signatures resulting from stress of nitride layer [5] (both on single layer of nitride on silicon and on the same nitride layer deposited on a product wafer). The nitride layers used in this study are dielectric films acting as isolation between metallic aluminum contact pads of patterned wafer. For some cases, changes in mechanical properties of this film can lead to yield issues of the devices (Fig. 6). The ellipsometry analysis was performed on the full wafer surface using point-to-point basic acquisition. The mapping grid used is composed of 6000 measurement points evenly spread on the 300 mm wafer surface, using a

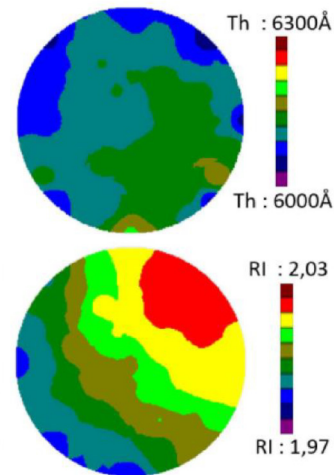


Fig. 7. In-line thickness and refractive index (at 633nm) spectroscopic ellipsometry measurement map on the nitride layer of the blanket wafer for refractive index (37 points).

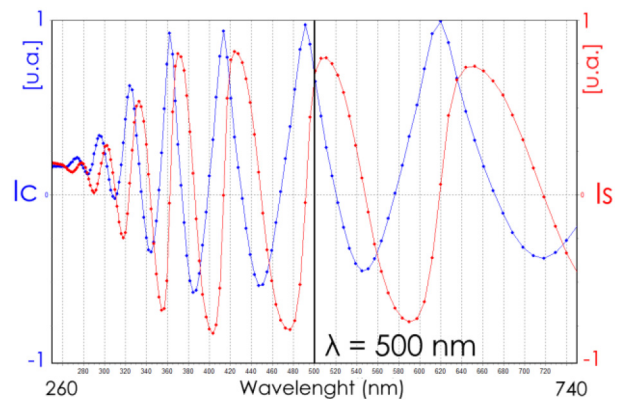


Fig. 8. I_c and I_s spectroscopic scan on the blanket wafer for the wavelength selection protocol.

spot size of 8 x 5 mm. Three and a half hours were necessary for a full wafer acquisition.

1) *Blanket Wafer Analysis*: Blanket nitride layers on silicon were first characterized by modeling with an industrial in-line ellipsometry system as already demonstrated in [6]. In this study, a strong inhomogeneity with a diametrical signature was detected in the refractive index of the layer, even though the layers thickness was relatively constant ($> 0.05\%$ variation) on the wafer surface (Fig. 7).

As a first step, we tested our model-less ellipsometry approach to characterize the same wafer. Following the basic protocol, a spectroscopic survey was performed at the center of the wafer in order to select the optimal wavelength for the further analysis. As it can be seen in Fig. 8, multiple wavelengths were eligible with comparable local slopes but in order to maximize luminous intensity from our source, a 500nm wavelength was retained.

The ellipsometry response at 500nm was collected using a dense mapping grid of 6000 points distributed evenly on the surface of the wafer are shown in Fig. 9. The intra-wafer signature cartographies obtained through model-less ellipsometry is extremely similar to the one obtained with the in-line

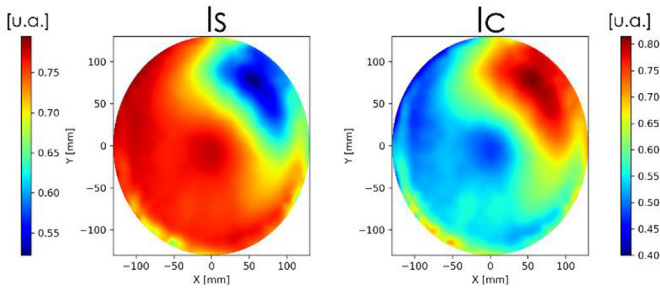


Fig. 9. Model-less ellipsometry images at 500nm (6000 points) of the same wafer studied in Fig. 7.

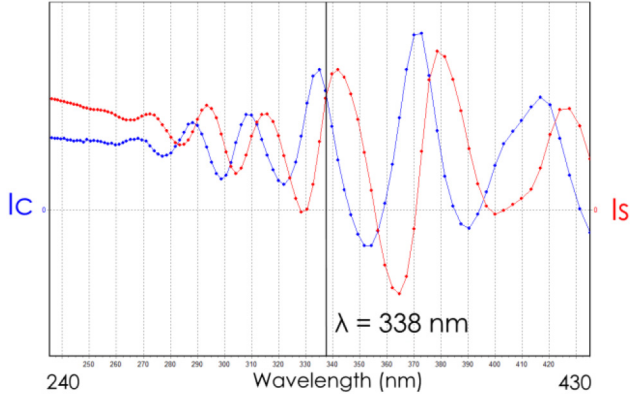


Fig. 10. Is and Ic spectroscopic scan on the patterned wafer for the optimal wavelength selection, which is 338 nm in this case.

measurements. This indicates the sensitivity of this approach to detect variation of the deposited film properties (induced by nitride stress in this case) without the need to develop a theoretical model. It is to be noted that thickness measurements were performed, and the signature displayed on the mapping does not correlate with the diametrical signature displayed by both industrial ellipsometry refractive index measurements, and model-less ellipsometry imaging results. This proves that our approach is, in this case, indeed sensitive to material properties variations.

2) *Product Wafer Analysis:* By contrast to blanket wafers, product wafers are composed of an intricate and complex stack of layers and patterns, for which an accurate ellipsometry model would be very arduous to produce and a model-less approach is more suitable. Metrology target structures used for in-line ellipsometry measurements are limited in number and especially rare at the extreme edge of the wafer, therefore, this kind of intra-wafer process variation would be hardly detectable by the usual process control solution.

As for blanket layers, the basic protocol of wavelength selection was applied, starting with a spectroscopic survey (Fig. 10). In this case, a large spot (8x5 mm) was used to average the optical signature of the underlying layers and a UV wavelength (338 nm) was selected for full wafer acquisition to focus sensitivity to the surface layer.

The same 6000 mapping previously used was utilized to gather the raw ellipsometric data, and the resulting images are displayed in Fig. 11a. A clear intra-wafer signature is observed along the diameter of the wafer, comparable with

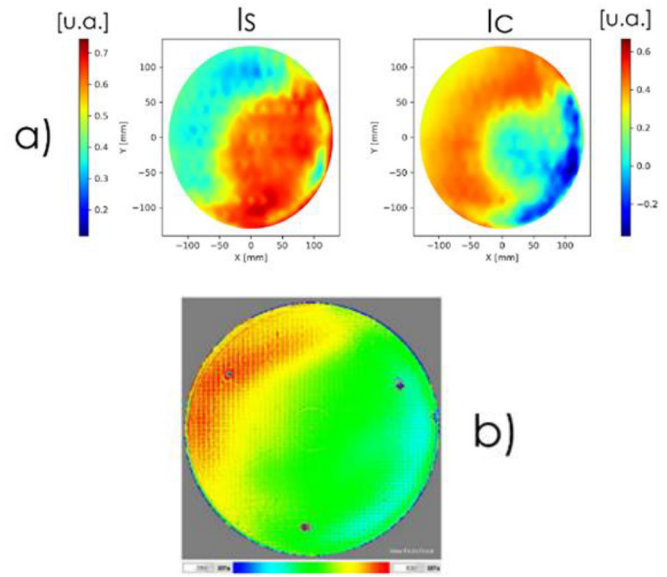


Fig. 11. a) Model-less ellipsometry images at 338nm (6000 points) and b) Interferometry stress cartography of nitride layer deposited on patterned wafer.

the one observed on the blanket wafer. It is to be acknowledged here that the orientation of the signatures can differ between blanket and product wafer due to the absence of notch alignment in the nitride deposition chamber. The results were compared to the characterization results obtained with a full wafer interferometry-based metrology technique which notably measures local stress and nano-topography [5]. The stress cartography is shown in Fig. 11b and displays an extremely similar signature with respect to the model-less ellipsometry ones.

In conclusion, we proved the sensitivity of our model-less approach to detect changes in material properties at the wafer scale, first on a blanket wafer, but more interestingly, on a product wafer. It is believed that variation in nitride properties during deposition can lead to changes in optical indexes and mechanical properties. Furthermore, a traditional industrial metrology ellipsometry process control solution which consists in measuring dedicated target would most likely not be able to detect these deviations, since these structures are sparsely distributed on the wafer. Our approach would need to be validated with more wafers with varying properties (e.g., thickness variation of underlying layers) to evaluate its robustness and reproducibility.

B. Color Resist Layers Intra Die Thickness Variation

For the second use case presented here, our intent was to detect intra wafer color resist thickness variation at deposition. The color resists are used as optical filters to perform RGB (Red, Green, Blue) pixel arrays for imagers devices. Due to complex topography effect on product wafers, the spin-coating deposition can lead to inhomogeneity in the resist thickness causing a radial striations signature. Those striations are then more pronounced at the edge of the wafer than the wafer center. They can be observed in optical images obtained from

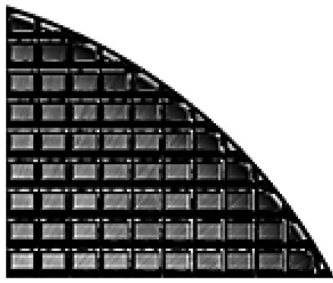


Fig. 12. Reflectometry image exhibiting the striations signature.

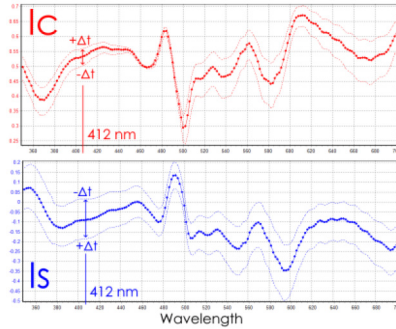


Fig. 13. Virtual subtract approach results, allowing for the wavelength selection.

reflectometry measurements in Fig. 12. For this case, where an improved resolution over a large surface is required, we applied our new protocol using a virtual layer for wavelength selection.

In this case, the first spectroscopic scan was performed before the color resist deposition, at the edge, where dies are likely to be affected by striations. Then, after deposition step, the same die was scanned again. The wavelength selection protocol results are presented in Fig. 13. Previous topological characterizations have established the average height of striations to 20nm, so this thickness variation was chosen for the virtual layer. This allows the measurement of signal variation induced on both I_s and I_c and a wavelength of 412 nm was chosen. Then, the advanced raster mode was used for acquisition, and the imaging ellipsometry results were compared to nanotopography mappings obtained from full wafer commercial interferometry equipment (Fig. 14).

In conclusion, we were able to detect a large-scale process deviation characterized by radial film thickness variations using a model-less ellipsometry approach on a product wafer, in the same way as the interferometry-based metrology technique. It is to be mentioned that this later equipment is limited to topography below 150nm and subsequently can suffer from reconstruction errors.

C. Periodic Etched 3D Structures Critical Dimensions Variation

The final case presented in this paper was to evaluate the sensitivity of our model-less ellipsometry imaging approach to variation in dimensions from periodic 3D vias (Fig. 15). We studied optical device wafers, which structures are trenches

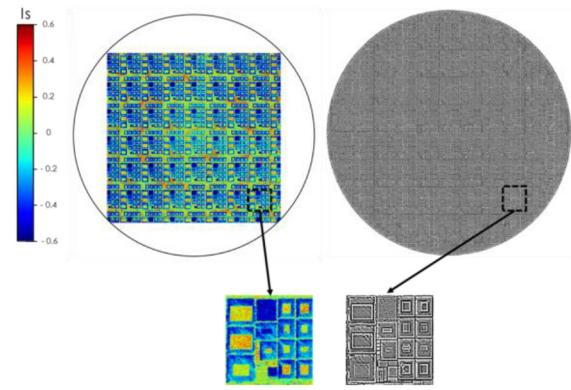
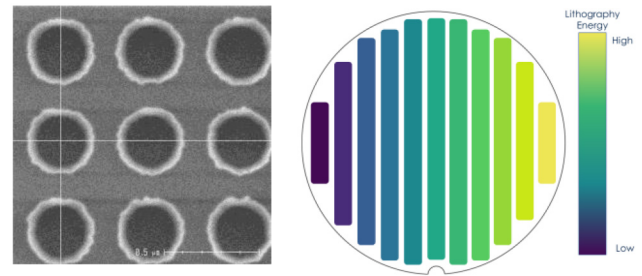
Fig. 14. Raster acquisition result (only I_s presented here) at 412 nm on the color resist wafer (~1.5 million points), compared with interferometry results.

Fig. 15. Example SEM images of periodic 3D structure used in optical devices wafers and energy matrix used during lithography wafer process.

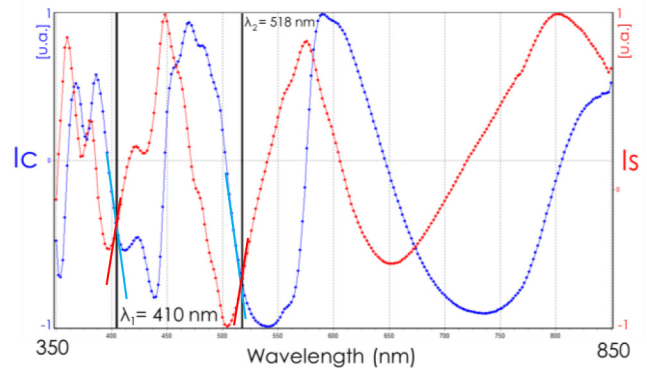


Fig. 16. Spectroscopic scan performed on the optical devices where two intercept points exhibit same local signal variations in intensity.

etched in order to adjust an incoming light beam's properties. The wafers used were processed with a diametrical energy matrix at the lithography step (Fig. 15). This allows for a linear variation of the critical dimensions of the etched vias along the horizontal diameter of the wafer.

The wafers are studied after the etching process step, and the basic wavelength selection protocol was used because no additional layer is deposited. The spectroscopic survey was performed on the optical devices, and two wavelengths with same local sensitivity (same local slope for I_s and I_c) were identified: 410 nm and 518 nm (Fig. 16).

The raster acquisition mode was then used to gather ellipsometry data with both selected wavelengths on a large area of the wafer, in order to evaluate its sensitivity to the trench's

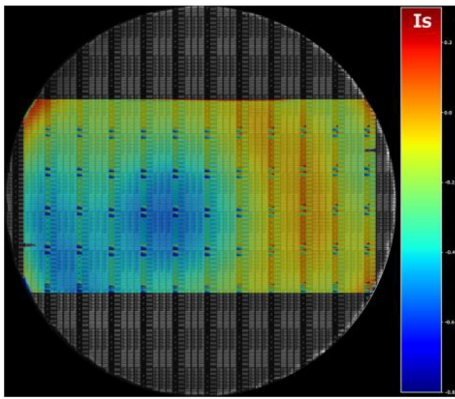


Fig. 17. Ellipsometry imaging result (I_s only) using raster acquisition protocol using the 410nm wavelength. (400,000 points).

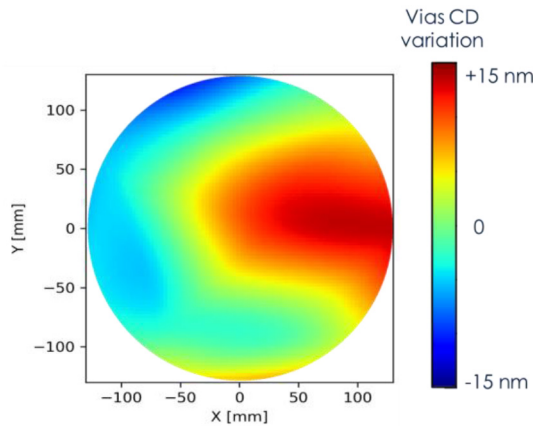


Fig. 18. Critical dimension (from interpolated 70 SEM-CD measurements – 37% variation from lowest to highest CD) mapping exhibiting both center/edge and energy matrix induced signatures.

dimensions variation. The results obtain from the ellipsometry imaging (only I_s for clarity) at 410 nm are presented in Fig. 17.

Unfortunately, the signature observed at this wavelength does not correlate perfectly with the critical dimension variation induced by the energy matrix measured by SEM-CD at 70 measurement points (interpolated wafer map of the CD variation on Fig. 18).

The second wavelength at 518 nm was then used, and the resulting image is shown in Fig. 19. Using this wavelength, we can now see a clear horizontal signature, along the energy matrix induced critical dimension variations, and a usual edge/center signature along the vertical axis. A full wafer acquisition at this wavelength is planned in order to confirm the sensitivity of our model-less imaging ellipsometry approach to this intended process variation.

The sensitivity difference of the images obtained with both intercept points clearly show the limitation of the basic approach for wavelength selection. It then becomes necessary to improve the selection of the proper wavelength for

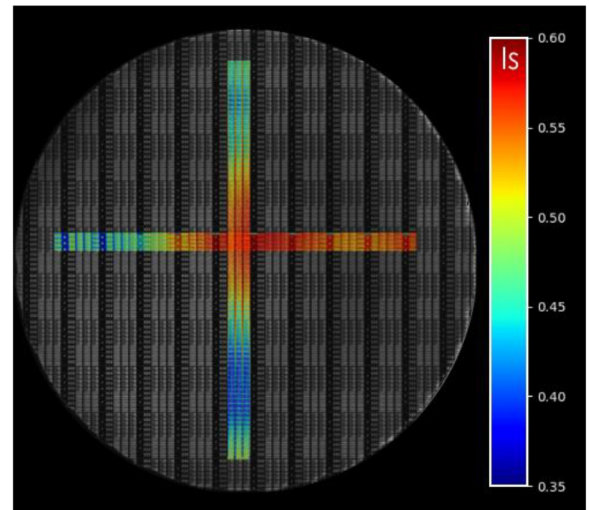


Fig. 19. Ellipsometry imaging (I_s only) result using raster acquisition protocol using the 518nm wavelength (83,000 points).

the image generation using the on-the-fly raster acquisition mode. It is considered that modeling the optical response of the metrology dies of the structure using Rigorous Coupled Wave Analysis (RCWA) will allow us to define new rules for the wavelength selection.

IV. CONCLUSION

The paper presents a proof of concept using an academic ellipsometry equipment to obtain raw data at a specific wavelength on the full surface of wafers, gathering them on the fly, in order to generate ellipsometry images. This model-less approach was capable of detecting various process deviations, on blanket and product wafers. It requires pre-characterization of the effect of the know process deviation on the ellipsometry response. In the case of film deposition variations, an innovative virtual layer approach is proposed to select the optimal wavelength for large-scale ellipsometry acquisitions.

REFERENCES

- [1] F. Anis, R. Gronheid, D. D. Van den Heuvel, and F. Zach, "Identifying contributors to overlay variability using a model-less analysis method," in *Proc. SPIE Metrol. Inspect. Process Control Semicond. Manufact.* XXXV, 2021, Art. no. 116111D.
- [2] M. E. Littau, C. J. Raymond, C. J. Gould, and C. Gambill, "Novel implementations of scatterometry for lithography process control," in *Proc. SPIE Metrol. Inspect. Process Control Microlithogr.* XVI, vol. 4689, 2002.
- [3] P. Braeuninger *et al.*, "Fast, Non-contact, wafer-scale, atomic layer resolved imaging of 2D materials by ellipsometric contrast micrography," *ACS Nano*, vol. 8, pp. 8555–8563, Aug. 2018.
- [4] O. Acher, E. Bigan, and B. Drévilion, "Improvements of phase-modulated ellipsometry," *Rev. Sci. Instrum.*, vol. 60, no. 1, pp. 65–77, 1989.
- [5] V. Brouzet *et al.*, "Full wafer stress metrology for dielectric film characterization: Use case," in *Proc. 30th Annu. SEMI Adv. Semicond. Manuf. Conf. (ASMC)*, 2019, pp. 1–7.
- [6] T. Alcaire, D. Le Cunff, V. Gredy, and J.-H. Tortai, "Spectroscopic ellipsometry imaging for process deviation detection via machine learning approach," in *Proc. 31st Annu. SEMI Adv. Semicond. Manuf. Conf. (ASMC)*, 2020, pp. 1–6.